Research Square

Preprints are preliminary reports that have not undergone peer review.
They should not be considered conclusive, used to inform clinical practice,
or referenced by the media as validated information.

Haplotype diversity and variant switching associated with long-term transmission and outbreak dynamics of Dengue virus 3 genotype III lineages

Rou Xuan Lee
Environmental Health Institute, National Environment Agency
Gladys Yeo
Environmental Health Institute, National Environment Agency
Carmen Koo
Environmental Health Institute, National Environment Agency
Vanessa Goh
Environmental Health Institute, National Environment Agency
Yee Ling Lai
Environmental Health Institute, National Environment Agency
Judith Chui Ching Wong
Environmental Health Institute, National Environment Agency
Lee Ching Ng
Environmental Health Institute, National Environment Agency
Hapuarachchige Chanditha Hapuarachchi
Chanditha_hapuarachchi@nea.gov.sg

Environmental Health Institute, National Environment Agency

Research Article

Keywords: Dengue virus, genomic surveillance, viral variant dynamics, haplotype diversity, lineage dynamics, molecular epidemiology, vector surveillance, outbreak risk assessment

Posted Date: September 23rd, 2026

DOI: https://doi.org/10.21203/rs.3.rs-10927088/v1

License: This work is licensed under a Creative Commons Attribution 4.0 International License.
Read Full License

Additional Declarations: No competing interests reported.

Abstract

Background

Dengue viruses (DENV) evolve rapidly, resulting in highly diverse virus populations with varying epidemic potential. Even though DENV lineage replacement events are common in hyperendemic regions, often associated with outbreaks, the underlying fine-scale evolutionary processes are not well-described.

Methods

We analysed 5,443 inter-host envelope gene consensus sequences and 171 complete genomes of DENV-3 genotype III collected weekly in Singapore between 2015 and 2025. These datasets were analysed (i). to characterize the temporal dynamics of population structure from clades to haplotypes (ii). To determine unique genetic features and selection pressure and (iii). To infer the correlation between haplotype diversity and reported case numbers and vector abundance.

Results

There were two distinct lineages (3III_B.1 [clade III] and 3III_B.3 [clade V]) that established long-term transmission, overlapping two outbreaks in 2019–2020 and 2022. Clade V was more common than clade III in 2019–2020 and was displaced by clade III in 2021, expanding exponentially during the 2022 outbreak. Despite variant diversity, only a single variant of each clade was dominant during respective outbreaks. The dominant variant of clade III showed the highest number of haplotypes and accumulated non-synonymous substitutions in a step-ladder pattern, whereas that of clade V maintained a less pronounced evolutionary profile during the study period. The overall haplotype diversity peaked during high transmission periods, in parallel to abundance of the vectors. There was a strong positive correlation between the number of haplotypes and the number of reported cases ($r = 0.72$, $p < 0.001$). Selection pressure analyses of the complete coding sequences indicated strong purifying selection, suggesting the stochastic evolutionary pattern of both lineages.

Conclusions

Variant switching and haplotype diversity are characteristic evolutionary processes associated with the transmission intensity and outbreak dynamics of DENV-3 lineages that sustain long-term transmission. By providing deep insights into temporal links between viral diversification, case burden and vector abundance, high-resolution genomic surveillance is valuable for outbreak risk assessment in dengue-endemic areas.

Highlights

- Single variant dominance in two DENV-3 genotype III clades was associated with lineage replacement during successive outbreaks in Singapore.
- Each clade maintained high diversity due to in-situ evolution and introductions during their long-term transmission.
- Overall haplotype diversity of two clades correlated positively with peaks in transmission intensity, reflected by high case burden and vector abundance.

- High-resolution genomic surveillance can support outbreak risk assessment in dengue hyperendemic settings.

Introduction

Dengue virus (DENV) is the most widespread arthropod-borne virus, inflicting approximately 400 million estimated infections annually [1]. More than half of the world population lives at risk of dengue. The virus is expanding its global footprint in parallel to the widening distribution of *Aedes spp* vectors due to climatic and ecological changes associated with global warming [2, 3]. Sustained non-sylvatic transmission of DENV requires the presence susceptible human hosts and competent vectors, mainly *Aedes aegypti* and *Aedes albopictus* as a secondary vector. Since the transovarial transmission does not play a major role in DENV propagation [4, 5], the virus relies heavily on the horizontal transmission that requires switching between a vertebrate host and an invertebrate vector.

The dual host switching, in turn shapes the evolutionary trajectory and adaptation of DENV to gain optimal fitness in each host. The low fidelity of RNA dependent RNA polymerase of DENV, and its fast replicative nature cause high mutation rates, generating a genetically diverse repertoire of variants that constitute natural DENV populations. These mutant spectra are regarded as phenotypic reservoirs, that dynamically change to gain better adaptability in virus populations [6, 7]. The constant evolutionary pressure affects the variant composition of DENV populations that tends to vary temporally and spatially, especially during period of high transmission intensity [8].

The in-situ evolution pronounced during such periods is largely shaped by the purifying selection and genetic drift that occur in both vertebrate and invertebrate hosts [9–11]. While purifying selection tends to purge unfavourable mutants, genetic drift causes selective sweeps resulting in the fixation of mutations that may or may not be adaptive to new host environments [11]. Consequently, lineage replacement events are common in dengue endemic regions, where they are often associated with outbreaks [12–14]. Empirical data indicates that these replacements occur at different levels of DENV diversity cascade, such as serotypes, genotypes and clades [15]. While various non-viral factors contribute to lineage dynamics [16, 17], lineage switching can also be attributable to a host-driven selection for enhanced fitness [18]. In this complex evolutionary landscape, the lineages that survive longer tend to demonstrate higher intra-lineage diversity than those that circulate for a short period. Therefore, recent computational advancements such as the DENcode framework have also highlighted the importance of integrating population level haplotype landscapes into transmission models [19].

DENV seems to have benefitted from the genetic plasticity provided by these evolutionary processes to succeed in establishing sustained transmission in a wide geographical range. Many tropical regions are currently hyperendemic to dengue, where all four serotypes of DENV circulate [2]. Likewise, dengue has been hyperendemic in Singapore for several decades, where alternating serotypes, genotypes and clades have been associated with successive outbreaks [20, 21]. From 2005, the dominant DENV serotypes oscillated between DENV-1 and DENV-2 till 2022, when DENV-3 became the dominant serotype. Based

on the available serotype data, DENV-3 has not been a dominant serotype in the country since late 1990s, which has also been reflected by the low seroprevalence for DENV-3 neutralisation antibodies in the population [22].

Despite improvements in genomic surveillance coverage in dengue endemic settings, there is limited literature on the long-term evolutionary dynamics of DENV lineages that contribute to epidemics in hyperendemic settings. The present study aimed to address this knowledge gap by analysing serially collected DENV genomic surveillance data in Singapore, where DENV populations have closely been monitored since 2006 to facilitate outbreak risk assessment. The study investigated the long-term temporal dynamics of two DENV-3 genotype III lineages associated with two outbreaks in Singapore during 2019–2022, aiming to (i) resolve their clade-to-haplotype population structure over time, (ii) compare substitution and selection patterns between lineages, and (iii) assess whether haplotype diversity co-varied with case burden and vector abundance. We hypothesised that the two lineages differ in intra-lineage haplotype composition, substitution patterns and temporal dynamics, and that overall diversity scales in parallel to transmission intensity.

Methods

Case surveillance

In Singapore, dengue is a legally notifiable disease, and all medical practitioners and clinical laboratories are required to report clinically suspected and laboratory-confirmed cases to the Communicable Diseases Agency (CDA) within 24 hours of detection. Laboratory confirmation is achieved through NS1 antigen, IgM antibodies or viral RNA detection by polymerase chain reaction (PCR). Only laboratory-confirmed cases are included in official surveillance statistics. Weekly case counts used in this study covered epidemiological weeks from 2015 EW01 to 2025 EW53 and were obtained from the arbovirus surveillance data, which is continuously updated from notified case reports by CDA (as of 30 June 2026).

Entomological surveillance

As part of Singapore's national *Aedes* surveillance programme, more than 70,000 Gravitraps have been deployed across high-rise public housing estates and landed homes. These sticky ovitraps target gravid female *Aedes* mosquitoes. The methodology for the trap placements, monitoring, data curation and interpretation is described elsewhere [23, 24]. Female *Ae. aegypti* abundances were quantified using the Gravitrap *Ae. aegypti* Index (GAI), defined as the mean number of adult females collected per functional Gravitrap per month. The quarterly averages were calculated from monthly GAI data.

Genomic surveillance

Genomic surveillance for arboviruses was carried out to analyse serotypes and genotypes of DENV in laboratory-confirmed patient sera on a weekly basis to provide timely situational awareness for dengue outbreak risk assessment and control in Singapore [25]. Established since 2006, local surveillance network includes more than 800 general practitioners, polyclinics, hospitals and commercial laboratories distributed across the country. In addition, adult mosquitoes captured in dengue clusters were also screened for DENV genomic testing on an ad-hoc basis. On average, serotyping and genotyping cover approximately 35–45% and 15–20% of all locally reported cases respectively in each year. Genotype surveillance includes the analysis of partial (envelope gene) and complete genomes to monitor the emergence of new virus lineages, their likely origin and local trends. It is aimed to provide insights into the cluster association and spatial expansion of emerging DENV variants in the country.

The dataset analysed in the present study included 5,443 complete envelope gene (*E*) sequences (1,479 bp) and 171 complete genomes of DENV-3 genotype III generated at the Environmental Health Institute, National Environment Agency, Singapore from 2015 to 2025 (see Additional files 1–3). The *E* gene sequences included those obtained directly from patient sera (n = 5,415) and 28 field-caught mosquitoes. All mosquito-derived *E* gene sequences were included in variant/haplotype classification and network analyses. They were subjected to the same filtering criteria as sequences from human samples. All complete genomes (n = 171) were generated from virus isolates obtained from patient sera. There were no complete genomes derived from mosquito samples. The complete genomes were used for Bayesian phylogenetic and mutation analyses.

Sequencing of DENV-3 envelope gene and complete genomes

Consensus *E* gene sequences were obtained directly from patient sera and mosquito homogenates. Complete genomes were generated from isolates obtained from patient sera. Viruses were isolated by using the *Ae. albopictus* C6/36 mosquito cell line (ATCC CRL-1660) as described elsewhere [26]. Viral RNA was extracted from sera using the QIAGEN QIAamp viral RNA mini kit (QIAGEN, Germany) according to manufacturer's recommendations. Viral RNA from mosquitoes was extracted as described previously [27]. DENV-3 typing, synthesis of complementary DNA (cDNA) and *E* gene and complete genome sequencing were done as described elsewhere [8, 20]. Raw nucleotide sequences were assembled using the DNABaser software package (SciVance Technologies, Germany).

Bayesian phylogenetic and phylodynamic analyses

Bayesian phylogenetic and phylodynamic analyses were conducted using complete polyprotein sequences of DENV-3 (10,173 nucleotides) to determine the genetic distinctness between study lineages and their evolutionary parameters such as the evolutionary rates and time to most recent common ancestor (tMRCA). The dataset included 171 study sequences and 179 sequences retrieved from NCBI nucleotide database to represent all non-sylvatic genotypes of DENV-3 reported in different regions across the globe. Each sequence in the final dataset (n = 350) was location and time tagged based on

the reported year and country (see Additional file 4). Here, sequences collected in the same year were treated as contemporaneous. Even though the year-level temporal granularity may broaden posterior uncertainty in substitution-rate and tMRCA estimates, limiting finer chronological precision, it is not expected to overturn the strong temporal signal and the tree topology.

Temporal signal of the final dataset was tested by using root-to-tip regression analysis (correlation coefficient and R^2) in TempEst version 1.5.3 [28] (See Additional file 5). The analysis showed a strong positive temporal signal (correlation coefficient = 0.97; R2 = 0.94), supporting molecular clock analysis (Supplementary Fig. 1). General time reversible substitution model with gamma distribution and invariant sites (GTR + F+Γ+I) was indicated as the best fitting nucleotide substitution model based on BIC criterion estimated using model finder in IQTREE2 [29] (see Additional file 6). The Bayesian phylogeny was constructed by using codon partition (1 + 2) and 3, log-normal Hamiltonian Monte Carlo relaxed molecular clock model and Bayesian SkyGrid tree prior (50 parameters in 3-year intervals) in BEAST X v10.5.0 software suite [30]. The log-normal relaxed molecular clock and a Bayesian SkyGrid tree prior were chosen to allow rate variation among lineages and not to assume a simple parametric demographic history expected in heterochronous DENV datasets. The BEAST run included 100 million Markov Chain Monte Carlo (MCMC) chains that were sampled at every 10,000 generations to ensure convergence above a minimum effective sample size (ESS) of 200 (see Additional files 7 & 8). The MCMC output was analysed using Tracer v.1.6 software (available at http://beast.bio.ed.ac.uk/Tracer). The maximum clade credibility (MCC) tree was constructed using TreeAnnotator v10.5.0 software and visualized in FigTree v.1.4.4 software (available at http://tree.bio.ed.ac.uk/software/figtree/) (see Additional files 9 & 10). Evolutionary parameters, such as evolutionary rates and time to most recent common ancestor (tMRCA), were calculated based on the MCC tree. The uncertainty in parameter estimates was expressed as 95% highest posterior density (HPD).

Estimation of case proportions contributed by circulating lineages using genomic surveillance data

Weekly lineage proportions and the corresponding numbers of reported dengue cases were estimated using a Bayesian state-space model fitted by Hamiltonian Monte Carlo in rstan [31] (see Additional files 11 & 12). Since not all reported cases are subjected to serotyping and genotyping, observed serotype counts and sequenced lineage counts were treated as nested multinomial samples of a shared weekly composition. Here, serotype data informed serotype shares, and genotype data informed lineage shares within serotype. Latent lineage states evolved as a first-order autoregressive process, and were mapped to the simplex with a softmax transformation. This summed lineage proportions to one, and lineage-specific case counts were obtained by multiplying weekly reported cases. This temporal structure allowed information to be shared across weeks when genomic surveillance was sparse. Four independent chains were run, each for 2,000 iterations, including 1,000 warmup iterations. Convergence was monitored using R-hat < 1.05 and bulk effective sample size > 400. Posterior means and 95% credible intervals are reported. The analysis included 58 DENV lineages detected during the study period

(574 weeks from 2015 EW01 to 2025 EW53) (see Additional files 13 & 14). Four MCMC chains achieved satisfactory convergence, with a median bulk effective sample size of 4,283, and a median R-hat of 1.001 (see Additional files 15–17). Weekly case numbers tagged to each lineage were calculated by multiplying the estimated weekly proportions by the total reported cases in each week.

Variant and haplotype classification, mutation profiling and diversity measures

All *E* gene sequences (n = 5,443) and complete genomes (n = 171) were aligned against the DENV-3 reference genome (NCBI Accession no. NC_001475) using MAFFT [32]. Variants were classified based on inter-host, consensus *E* gene sequence clusters sharing 100% nucleotide identity, generated by using CD-HIT [33]. The single nucleotide polymorphism (SNP) patterns of each variant were confirmed by visualizing in BioEdit v7.2.5 [34]. These patterns were extracted using SNP-sites [35].

Each variant was further classified into haplotypes using a hierarchical scheme cascading from wild type (WT). The WTs comprised sequences identical to the first sequence of each clade detected through local surveillance (prototype strain). Accordingly, the WT served as the basal reference for SNP calling. Haplotypes possessed at least one unique SNP relative to the WT of each variant (see Additional files 18 & 19). Each haplotype included at least five identical sequences as operational evidence that haplotype-defining SNPs were recurrent and "putatively fixed" in the dataset. The suitability of this numerical threshold was further evaluated through a sensitivity analysis at thresholds 3, 5 and 10 sequences using the *E* gene alignment. This analysis produced the same qualitative temporal patterns of haplotype predominance and expansion at each threshold evaluated, supporting retention of the ≥ 5 threshold. Haplotypes had either founder SNP patterns alone or additional SNPs labelled with nested identifiers to reflect successive mutational steps within each variant (Supplementary Tables 1 and 2). In this variant-haplotype nomenclature, SNP patterns follow a parent-delta convention. The variant-specific SNPs are founder SNP(s) shared by all haplotypes within that variant. The haplotype-specific SNP/s are the additional SNP(s) that distinguish a given haplotype from its immediate observed parent in the nested hierarchy. Accordingly, the complete SNP profile of any haplotype consists of (i) the variant founder SNP(s) and (ii) the haplotype-specific SNP(s) accumulated along its nested path (for example, haplotype 5.1.1 = V5 founder SNP[s] + 5.1-specific SNP[s] + 5.1.1-specific SNP[s]). Sequences carrying singleton SNPs (observed in fewer than five sequences) were excluded from the haplotype analysis.

Non-synonymous mutation profiling was done by using the complete polyproteins of study sequences. They were aligned and compared against 1,481 complete coding sequences of DENV-3 genotype III retrieved from NCBI (as of 07 Apr 2026) using BioEdit v7.2.5 [34] to assess their uniqueness, global prevalence and distribution.

Haplotype network construction and visualization

The longitudinal evolutionary pattern of the emergence and expansion of different variants was determined by using a maximum likelihood phylogenetic tree constructed and visualized using the Nextstrain pipeline [36]. The analysis was done using only the first and last detected sequences of each category - WT (n = 4), variant and/or haplotype (n = 236) of clades III and V. This selection was done to retain the temporal signal, while reducing redundancy from identical sequences within WTs, variants and haplotypes to illustrate the in-situ evolutionary pattern of each clade rather than to estimate demographic parameters. Analyses were run with default Nextstrain settings.

The genetic relationships between haplotypes within each clade were visualized using separate minimum spanning tree networks. Firstly, a genetic distance matrix was constructed by calculating the symmetric difference between the sets of unique SNPs for all pairs of haplotypes in each clade. The minimum spanning network topology was inferred using each SNP distance matrix to identify the parsimonious links connecting all observed haplotypes. Barnes-Hut simulation algorithm [37] was used only for positioning of nodes based on precomputed topology, which was visualized via the pyvis framework [38] to provide a spatial representation of the variant and haplotype landscape. Node sizes were scaled proportionally to the square root of the sequence count for each haplotype to represent their relative prevalence and temporal emergence. The edge thickness and transparency were weighted inversely to the SNP distance to emphasize closely related genetic transitions.

Selection pressure analyses

Site-level selection was assessed on a single alignment of 171 complete polyprotein sequences (10,173 nucleotides) of clades III and V because both lineages belong to DENV-3 genotype III and the number of clade V complete genomes (n = 37) was limited for robust codon-level inference. Analyses were implemented in Hyphy 2.5 [39] using a phylogeny inferred using IQTREE-2 [29]. Purifying selection at individual codons was inferred using single-likelihood ancestor counting (SLAC) [40], fixed effects likelihood (FEL) [40], and fast unbiased Bayesian approximation (FUBAR) [41] methods. Sites were considered significant at $p \leq 0.1$ for SLAC and FEL (as a screen for constrained sites in viral genomes), and at posterior probability ≥ 0.90 for FUBAR (as the principal Bayesian support for purifying selection). Episodic diversifying (positive) selection at individual codons was also assessed (significance threshold $p \leq 0.1$) as an additional method using the mixed effects model of evolution (MEME) [42]. These cut-offs were chosen to be consistent with common HyPhy practice for exploratory codon models. More stringent, conventional cut-offs, such as $p \leq 0.05$ may reduce power when diversifying selection is much weaker than purifying selection. Tajima's D and associated P-values (beta approximation) were calculated separately for the complete polyprotein sequences of each clade in R using the pegas package [43] as a complementary summary statistic of allele-frequency spectra that may reflect purifying selection, demographic expansion, or both.

Statistical analyses

To evaluate the relationship between the Gravitrap *Ae. aegypti* index (GAI), number of reported cases and viral genetic diversity, we performed a correlation analysis between quarterly mean GAI (36 quarters

from Q1-2017 to Q4-2025), number of reported cases (44 quarters from Q1-2015 to Q4-2025) and the number of haplotypes in both clades from Q1-2015 to Q4-2025. Pearson's product-moment correlations were calculated as the primary metric between haplotype counts and reported cases as well as GAI, with two-tailed p-values calculated to determine significance at $p < 0.05$, because the analysis targeted approximately linear co-variation among continuous quarterly summaries. Spearman's rank correlations were also calculated as a secondary metric. Here, consecutive quarters are temporally autocorrelated, and as such parametric p-values that assume independence may be anti-conservative. Therefore, correlations were interpreted as descriptive measures of contemporaneous co-variation. Linear trends were visualized with ordinary least-squares regression, with 95% confidence bands obtained via the default bootstrap procedure in Seaborn's regplot. Temporal precedence was assessed by recomputing correlations with predictors lagged by 1–4 quarters relative to GAI or haplotype counts leading reported cases, and vice versa.

The number of *E* gene sequences analysed in each quarter (Q1 = EW1–13, Q2 = EW14–26, Q3 = EW27–39, Q4 = EW40–53) for clade III and clade V from 2015 to 2025 was derived to evaluate whether quarterly haplotype counts were influenced by sequencing effort. The analysis used (i) the number of sequences analysed, (ii) the haplotype count used in the transmission–diversity analyses, (iii) haplotypes per 100 sequences, and (iv) residuals from an ordinary least-squares regression of haplotype count on the number of sequences for each quarter. Pearson and Spearman correlations were calculated for associations among sequencing effort, raw and effort-adjusted haplotype counts, reported cases and GAI. All analyses were implemented in Python using the SciPy and Seaborn libraries.

Ethics statement

DENV-3 *E* gene sequences were generated as part of the National Environment Agency-Ministry of Health (now Communicable Diseases Agency), Singapore joint arbovirus surveillance programme. The permission has been obtained to use the aggregated genomic surveillance data for the publication. The complete genome sequences were generated under the IRB003.1 approved by the institutional review board of the Environmental Health Institute, National Environment Agency, Singapore.

Results

Two outbreak lineages were genetically distinct clades of DENV-3 genotype III that have established long-term transmission in Singapore

Bayesian phylogenetic analysis using complete coding sequences showed two genetically distinct lineages of DENV-3 genotype III (Fig. 1); 3III_B.1 and 3III_B.3 based on the Nextclade nomenclature system (Aksamentov et al., 2021; Hill et al., 2024). They were hereafter named as clade III and clade V and were first detected in Singapore in April 2015 and December 2017 respectively. In tree topology, clade III sequences formed a monophyletic group, whereas clade V sequences split into two monophyletic groups, and included a related lineage (3III_B.3.2) that emerged in the Americas [44] and the Caribbean [45] in early 2020s as well as Asian sequences (see Additional file 20). Clades III and V

were distinguishable based on their genome-wide substitution profiles - each including eight amino acid differences (Fig. 1). Even though not genetically identical to either clade, DENV-3 genotype III sequences with amino acid profiles specific to each clade have also been reported in Asia [46], and Americas [44, 45], where they have caused significant epidemiological shifts and explosive outbreaks. These observations showed that two local clades are genetically distinct lineages that share a common ancestry with lineages circulating elsewhere (Fig. 1). The median tMRCA of clade III was 2012.8 (95% HPD: 2011.9-2013.6) and that of clade V was 2009.5 (95% HPD: 2008.1-2010.7), based on median node heights [clade III: 13.20 and clade V: 16.80 years before the most recent tip (2026)] of MCC tree. The mean substitution rate was 6.59 x 10^{-4} substitutions/site/year [95% highest posterior density (HPD): 6.22–6.98×10 − 4], which was consistent with empirical estimates [47, 48]. Overall, our analysis showed that lineages related to clade V have been more widespread globally than those related to clade III. Both clades were continuously detected among surveillance samples after the emergence in Singapore, suggesting their sustained autochthonous transmission during the study period.

Singapore experienced three outbreaks during the study period. The 2016 outbreak (13,085 cases) was associated with a switch in predominant serotype from DENV-1 to DENV-2. It was followed by a lull period from 2017 to 2018 when DENV-1, 2 and 3 cocirculated at different proportions. DENV-2 became the predominant serotype again in 2019, igniting a 2-year outbreak (15,979, cases in 2019 and 35,210 cases in 2020), during which both DENV-3 clades also circulated; mainly clade III in 2019, and clade V in 2020. This outbreak subsided in 2021, but a switch from DENV-2 to DENV-3 in mid-2021 triggered another outbreak in 2022, with 32,154 cases (Fig. 2). This outbreak was preceded by the replacement of the previously dominant DENV-2 lineage by clade III (Fig. 2). This shift in clade dominance within DENV-3 occurred approximately 10–12 months before peak transmission in 2022, indicating that changes in lineage composition temporally preceded the outbreak peak. Nevertheless, clade III was replaced in mid-2023 by the same DENV-2 lineage that was dominant during 2016 and 2019–2020 outbreaks (Fig. 2), although this later switch was not followed by a large outbreak as in prior years.

Clade III and clade V consisted of 10 monophyletic variants that included multiple haplotypes, demonstrating a strong and long-term in-situ evolutionary process

Among 5,443 DENV-3 *E* gene sequences analysed, 4,657 (85.5%) belonged to clade III, of which 77.3% (n = 3,598) were reported in 2022, highlighting its dominant role during the 2022 outbreak. The remaining sequences (n = 786) belonged to clade V. Based on founder SNP combinations relative to the WT of each clade, seven variants (V1-V7) were identified in clade III and one variant (V1) in clade V (Table 1), indicating 10 monophyletic groups in two clades (Table 1). Each variant comprised one or more haplotypes that shared the variant-defining founder SNP(s); haplotype SNP profiles are provided in Supplementary Tables 1 and 2.

Table 1
Summary of variants and associated haplotypes in clades III and V

Clade	Monophyletic group	No. of haplotypes[#]	No. of sequences
Clade III	WT	0	23
	V1	1	36
	V2	0	13
	V3	0	17
	V4	0	13
	V5	87	4,536
	V6	0	7
	V7	1	12
Clade V	WT	0	23
	V1	23	763

[#]Zero values for variants indicate that there was no further haplotype subdivision in respective variants. Wild type strains include sequences that were identical to those detected first for each clade (prototype strains). Therefore, strains carry no SNPs as compared to variants (no haplotypes). The haplotype SNP profiles are provided in Additional files 18 and 19.

Clade III included a substantially higher number of haplotypes (n = 89) than clade V (n = 23). Variants with the highest number of haplotypes represented the highest proportion of sequences of each clade, and demonstrated a step ladder tree topology, consistent with in-situ evolution shaping the diversity within each clade over time (Fig. 3). Notably, there were 10 amino acid substitutions between the WT and variant 1 of clade V sequences (see Additional file 21), suggesting that variant 1 of clade V was more likely to have emerged through an independent introduction, instead of descending from WT strains.

The greatest expansion of haplotypes occurred during the 2019–2020 and 2022 outbreaks, coinciding with peak periods of transmission (Fig. 4). There was a strong, statistically significant positive linear association [49] between quarterly reported cases and haplotype counts of both clades across 44 quarters from 2015 Q1 to 2025 Q4 (Pearson's $r = 0.72$; $p < 0.001$; Spearman's $\rho = 0.73$; $p < 0.001$) during the study period (see Additional file 22).

Integration of vector surveillance data showed that haplotype expansion also coincided with peaks in *Ae. aegypti* abundance, reflected by the Gravitrap *Ae. aegypti* Index (GAI). The correlation between GAI and haplotype counts was moderate but statistically significant across 36 quarters from 2017 Q1 to 2025 Q4 (Pearson's $r = 0.49$, $p = 0.002$; Spearman's $\rho = 0.56$, $p < 0.001$). Even though GAI was in an increasing trend during the 2019–2020 and 2022 outbreaks (Fig. 4), lagged correlation analysis did not support a

consistent lead of GAI over cases. Associations between GAI and cases were strongest when cases led, or were contemporaneous (Spearman ρ = 0.45, *p* = 0.006; Pearson r = 0.29, *p* = 0.088 at lag 0). GAI leading cases by 1–4 quarters was not significant by Pearson (r = 0.13–0.20, all p > 0.27), and only the one-quarter lead reached nominal significance by Spearman (ρ = 0.36, *p* = 0.032). Haplotype counts correlated most strongly with cases in the same quarter (Pearson r = 0.72; Spearman ρ = 0.73; both p < 0.001). However, a one-quarter lead of haplotype counts remained significant but weaker (Pearson r = 0.48, *p* = 0.001; Spearman ρ = 0.61, p < 0.001). The reverse lag showed a comparable magnitude (Pearson r = 0.55; Spearman ρ = 0.69; both p < 0.001) (Supplementary Table 4). Quarterly haplotype counts were strongly associated with sequencing effort (sampling intensity) across quarters with at least one sequence (Pearson's r = 0.90, p < 0.001; Spearman's ρ = 0.91, p < 0.001). Reported cases were also correlated with the number of sequences analysed (r = 0.65; ρ = 0.68; both p < 0.001). After adjusting for sequencing effort, cases were moderately correlated (Pearson's r = 0.29, *p* = 0.074; Spearman's ρ = 0.47, *p* = 0.002) with haplotype residuals (observed haplotype count-count predicted from n sequences). GAI was not significantly associated with haplotype residuals (Pearson's r = 0.12, *p* = 0.52; Spearman's ρ = 0.17, *p* = 0.35) (see Additional file 23). Accordingly, contemporaneous correlations between raw haplotype counts and cases or GAI reflected transmission intensity and sequencing effort rather than viral diversification alone. Therefore, even though haplotype richness and GAI increased with transmission intensity, the quarterly correlation analyses did not establish that either GAI or haplotype counts consistently precede outbreaks nor that vector abundance caused viral diversification. Taken together, the findings indicate temporal co-variation among cases, *Ae. aegypti* abundance and haplotype diversity during high-transmission periods.

Most common variants of both clades established long-term transmission, but a single variant became dominant in 2020 and 2022

Temporal analysis using *E* gene sequences of clade III (n = 4,657) and clade V (n = 786) revealed distinct survival pattern of constituent variants (Fig. 5). The most common variants of both clades emerged during periods of relatively low transmission intensity and survived the longest period. During the 2019–2020 outbreak, clade V (variant 1) was more prevalent than clade III (V5-V7). Of those clade III variants (V5-V7), only variant 5 could be detected beyond 2020, replacing clade V variant 1 as the predominant DENV-3 variant by mid-2021 - a lull period of case burden. This variant replacement coincided with observed serotype switch from DENV-2 to DENV-3 in 2021. Subsequently, the proportion of clade III variant 5 increased markedly when transmission intensity escalated in 2022. These observations suggested that the replacement of a single variant overlapped with a shift in serotype dominance prior to the major outbreak that year. Despite occurring during a period of low transmission intensity, it was not clear whether the variant turnover was due to competitive displacement, stochastic loss or any other attributable factors related to population processes.

Step-ladder pattern of non-synonymous substitutions distinguished clade III evolutionary dynamics

The analysis of complete coding sequences of both lineages (134 clade III and 37 clade V sequences) revealed distinct temporal emergence of non-synonymous substitutions within each clade (Fig. 6). Clade III accumulated a greater number of amino acid changes than clade V, and they predominantly appeared within the most prevalent variants of each clade. Clade III displayed a strong founder effect followed by progressive, step-ladder accumulation of substitutions within the dominant variant, consistent with an in-situ evolutionary pattern (Fig. 6). Notably, clade III acquired these substitutions before its subsequent expansion during 2022 outbreak. On the other hand, additional substitutions emerged in clade V genomes after the 2020 transmission peak. Importantly, the WT and variant 1 of clade V differed by multiple non-synonymous substitutions (Supplementary Table 3), suggesting that variant 1 likely emerged through an independent introduction rather than descending from WT strains. Weak in-situ evolutionary signal in clade V was also supported by the lack of founder effect in substitution patterns (Fig. 6). This was temporally consistent with separate introductions in 2021 and 2024, rather than step-ladder evolution within the dominant 2019–2020 variant. Taken together, non-synonymous substitution patterns highlighted a distinct intra-clade substitution pattern for clade III relative to clade V during local circulation.

However, these substitutions in both clades were not accompanied by genome-wide evidence of pervasive diversifying selection (Table 2). Instead, selection pressure analyses supported largely purifying evolution, despite episodic, site-specific signals detected only by MEME, but not supported as diversifying by the other pervasive-selection methods. Tajima's D, calculated separately for each clade, was also negative for clade III (− 2.05; n = 134; $p = 0.02$) and clade V (− 0.87; n = 37; $p = 0.41$). The significantly negative value for clade III aligns with purifying selection, but may also arise from demographic expansion or other population processes, and therefore cannot be directly interpreted as evidence of selection [50]. In contrast, clade V did not indicate a significant departure from neutrality.

Table 2
Site-level selection analyses of the combined complete coding sequences of clades III and V (n = 171)

Method	No. of sites under diversifying selection	No. of sites under purifying selection
SLAC	0	73
FEL	0	264
FUBAR	0	856
MEME	11[£]	Not applicable

[£]Codons with episodic diversifying selection by MEME ($p \leq 0.1$): E-137, E-367, NS1-256, NS4A-15, NS2A-28, NS2A-60, NS3-185, NS4A-46, NS5-23, NS5-129, and NS5-414. E = envelope; NS = non-structural proteins. MEME does not infer purifying selection.

Discussion

Dengue virus populations are known to be highly diverse and dynamic. Their compositions are determined by a myriad of factors related to DENV's complex transmission cycle that requires the virus to be competent in a vertebrate and invertebrate host. Being an RNA virus, DENV demonstrates relatively a high mutation rate due to several factors such as poor proof-reading ability of its RNA dependent RNA polymerase [51] and its small single-stranded genome [52]. Consequently, many mutants emerge when the virus replicates in both hosts [53, 54]. The resultant mutant spectra constitute a quasispecies population structure [55], which may be beneficial to the virus to survive in different host environments in successive transmission cycles. These mutant spectra may differ in phenotypic properties [56]. Changes in the relative frequency of co-circulating variants contribute to the overall composition and dynamic nature of DENV populations in nature, although the driving mechanisms remain incompletely resolved. Therefore, understanding the micro-evolutionary processes that shape DENV populations is important but not well-described. Many previous descriptions of DENV evolution primarily focus on the macro-level of diversity cascade that includes serotypes, genotypes and less commonly clades. Variant level descriptions are scarce, mainly due to not having enough data to perform in-depth analyses at high genetic resolution. In this context, the present study aimed to provide an in-depth view of temporal dynamics of DENV-3 variant diversity by analysing a large serial (weekly) collection of *E* gene sequences and a representative collection of complete genomes from 2015 to 2025. The findings reflect the fine granularity of genetic composition of two DENV-3 clades that were circulating in Singapore for a long period. While the observations illustrate that the genetic diversity of natural DENV populations are much higher than what is captured through macro-scale genetic analyses, they also highlight the vast nature of genetic changes that take place constantly during in-situ evolution of DENV lineages in endemic settings. These findings may have important implications for vaccine development studies and novel vector control strategies such as *Aedes-Wolbachia* replacement approach [57, 58]. Recent studies have shown that the antigenic distance between different lineages differs within and between DENV serotypes, which determines the varying degree of neutralizing ability of a previous exposure to DENV and clinical severity [59, 60] as well as their epidemic potential [61]. Likewise, variant diversity and background evolutionary mechanism may act against the odds of *Aedes-Wolbachia* replacement success, by selecting variants that could modulate the level of inhibitory effects on virus replication in vectors carrying *Wolbachia* either individually or collectively as a quasispecies ensemble [62]. These observations therefore demonstrate that macro-scale genetic classifications alone ignore the micro-evolutionary processes that determine the epidemiological behaviour of virus lineages.

In agreement with empirical data, the study findings showed that transmission intensity and length of survival of a particular lineage are associated with its fine-scale genetic complexity [63, 64]. In our findings, the haplotype diversity was highest in the long-surviving variants in each clade. Moreover, the haplotype expansion mainly occurred during periods of intense transmission in a positively correlated manner, suggesting that micro-scale genetic heterogeneity may be a useful proxy for transmission intensity. This may have an extended utility in predictive modelling for dengue that largely relies on climate variables and serotype dynamics [65]. However, the associations reported herein are temporal and do not establish that genetic diversification forecasts outbreaks. Haplotype-informed approaches

[19] further suggest that genetically diverse virus populations may behave differently when host immunity and vector abundance fluctuate. This notion is also supported by our findings that haplotype expansion coincided with peaks in the Gravitrap *Ae. aegypti* Index (GAI), which rose sharply during high transmission periods. The 2019–2020 and 2022 outbreaks occurred when GAI was in an increasing trend, indicating a close association among vector abundance, case burden and haplotype richness. However, this does not confirm that vector proliferation caused viral diversification. Furthermore, the temporal analyses also showed that a single variant of long-surviving DENV lineages accounted for the majority of samples sequenced. Among all variants of clades III and V, dominant variants were the key attributes of DENV-3 transmission during 2019–2020 and 2022 outbreaks respectively. Of them, the dominant variant of clade III contributed to as high as 90% of transmission in 2022. Interestingly, the haplotype diversity reduced drastically from its peak in 2022 together with cases and *Ae. aegypti* abundance (GAI). The reduction in GAI reflected the effectiveness of the integrated vector surveillance programme in Singapore [25], especially Project Wolbachia, which has been progressively expanded since 2016 to suppress local *Ae. aegypti* population [66, 67]. The findings therefore indicate how effective the vector control measures in mitigating DENV transmission, and how virus population dynamics can be used as a tool to monitor the effectiveness of dengue control programmes. These aspects testify the importance of genomic surveillance and in-depth data analyses to support outbreak risk assessment, especially in larger countries/regions [68]. In contrast to Singapore, where DENV transmission presumably occurs in a tightly knit dispersal network due to its small size and a well-connected transport system, the insights gained through in-depth molecular epidemiological analyses could further facilitate strategic resource planning during epidemics in large countries, where transmission networks are likely to be disconnected due to geographical barriers and limited human movement. Understanding the emergence and epidemic behaviour of different variants and the dispersal of variants with high epidemic potential to “new” areas are important components of outbreak risk assessment in such settings [68].

Beyond viral diversity and vector abundance, lineage switching and replacement also coincide with broader host-level dynamics and environmental factors. Sero-epidemiological studies in Singapore indicate a long-term decline in dengue’s force of infection (FOI), stabilizing near 10 infections per 1,000 persons annually since the mid-1990s [69, 70]. While this FOI trend reflects successful vector control, it has also lowered background immunity, particularly serotype-specific protection among younger cohorts [22, 71]. This immunity gap was evident during the 2022 DENV-3 outbreak, when clade III viruses rapidly became dominant. These observations highlight the role of immunological and ecological factors in DENV evolution, even in the absence of selective pressures. It is known that lineage success depends on local ecological and host contexts [72, 73]. Moreover, vector competence also plays a pivotal role in lineage success [74], especially under favourable climatic conditions [75, 76]. Moreover, phenotypic plasticity of mosquito populations may influence the outbreak behaviour of virus traits [77]. These observations highlight the importance of integrating genomic surveillance data into the understanding of connectivity between host immunity, epidemic behaviour, vector biology and local ecological context for

outbreak risk assessment, because a lineage successful in one country may not necessarily achieve similar epidemic potential elsewhere.

In contrast to clade V, clade III accumulated seven non-synonymous substitutions in an in-situ evolutionary pattern [78] with strong founder effect. All of these non-synonymous substitutions were in non-structural proteins (NS1, NS2A and NS3). Non-structural proteins of DENV mainly encode for the functional elements such as those required for virus replication [79]. Besides, NS1 and NS3 have also been implicated in immune modulation, replication and pathogenicity [80–83]. Although purifying selection was the predominant force, the contrasting evolutionary dynamics between two clades highlight different adaptive patterns that may have contributed to differences in phenotypic and epidemic behaviour between them - a possibility of interest for future experimental studies. Importantly, unlike clade V, clade III accumulated all non-synonymous substitutions by mid-2021, prior to its explosive expansion in 2022. Therefore, it is worth investigating whether these substitutions altered the phenotype or transmissibility of clade III to explain its observed epidemic potential. Although the case fatality rate during this outbreak remained low, further studies on correlation between viral genetic variation and clinical outcomes are also critical to understand how evolutionary changes may influence dengue pathogenesis and severity.

This study included several limitations. Firstly, a relatively lower number of complete genomes was analysed as compared to the large collection of *E* gene sequences. This was because DENV genotypes are largely characterized by using *E* gene sequences in the genomic surveillance programme in Singapore. Complete genome sequencing is done using isolates obtained from a subset of clinical samples selected based on *E* gene-based genotype findings. Nevertheless, complete genomes of clades III and V were generated from serially collected samples since their first detection, so that the analysed dataset is expected to reflect the non-synonymous substitution patterns in both clades. Complete genomes were also likely to have provided higher resolution on variant definitions and thereby a more comprehensive evolutionary profile of both clades than *E* gene sequences. A further limitation is that haplotype richness estimated from genomic surveillance data is dependent on sampling intensity. The strong correlation between quarterly haplotype counts and the number of sequences analysed shows that raw haplotype totals are dependent at least partially on sequencing effort, especially when genotyping volume increased during high-transmission periods. Effort-adjusted analyses moderated associations between haplotype diversity and cases and GAI. The findings therefore indicated that haplotype counts may be a joint marker of transmission intensity and surveillance intensity. Importantly, conclusions regarding variant switching, hierarchical haplotype structure and clade-specific substitution trajectories are based on sequence relationships and mutational pathways rather than only on raw quarterly haplotype totals. Furthermore, the inferences on “quasispecies” population structure should ideally be supported by intra-host sequencing data [84]. Instead, the present study described the inter-host haplotype diversity using clinical samples collected weekly, that showed the existence and fluctuations of multiple variants and haplotypes at a given time, suggestive of a “quasispecies-like” population structure. This warrants further studies on the intra-host diversity analyses using next

generation sequencing technology to determine the contribution of dominant variants to the “quasispecies” structure of natural DENV populations [85].

Conclusions

The present study indicates that variant- and haplotype-level dynamics and turnover among co-circulating variants are long-term transmission characteristics of DENV lineages associated with outbreaks. The findings reinforce the need for robust, country-specific genomic surveillance frameworks that integrate case, seroprevalence and vector data to improve outbreak risk assessment and resource planning in dengue-hyperendemic settings.

Declarations

Acknowledgements

We thank colleagues at the Environmental Health Institute (EHI), National Environment Agency, and Communicable Diseases Agency, Singapore for their support in the arbovirus surveillance and entomological surveillance programmes. We specially thank Dr. Chia-Chen Chang at EHI for her advice on the Bayesian state-space model used for the estimation of case proportions contributed by circulating lineages.

Author Contributions

RXL: Formal analysis, Data curation, Visualization, Writing – original draft; GY: Data curation, Writing – original draft; CK: Data curation, Writing – review & editing; VG: Methodology, Data curation, Writing – review & editing; YLL: Data curation, Writing – review & editing; JCCW: Resources, Writing – review & editing, Supervision, Project administration; LCN: Resources, Writing – review & editing, Supervision, Funding acquisition; HCH: Conceptualization, Methodology, Formal analysis, Writing – original draft, Visualization.

Conflict of Interest

Authors declare no conflict of interest pertaining to this publication.

Data Availability Statement

The DENV-3 genotype III *E* gene sequences and complete genome sequences generated in this study have been deposited in the NCBI GenBank database under accession numbers PZ585783 - PZ585953 (complete genomes), PZ587777 - PZ590376 and PZ590399 - PZ593126 (*E* gene, n = 5,328; 115 *E* gene sequences are captured in 171 complete genomes). All additional files can be accessed through DOI: 10.6084/m9.figshare.33413509.

Funding source

This study was supported by the National Environment Agency, Singapore. The funding source had no role in the study design, data collection, data analysis, data interpretation, writing of the report and the decision to submit the article for publication.

References

1. Bhatt S, Gething PW, Brady OJ, Messina JP, Farlow AW, Moyes CL, et al. The global distribution and burden of dengue. Nature. 2013;496:504–7. https://doi.org/10.1038/nature12060.
2. Messina JP, Brady OJ, Golding N, Kraemer MUG, Wint GRW, Ray SE, et al. The current and future global distribution and population at risk of dengue. Nat Microbiol. 2019;4:1508–15. https://doi.org/10.1038/s41564-019-0476-8.
3. Paz-Bailey G, Adams LE, Deen J, Anderson KB, Katzelnick LC, Dengue. Lancet. 2024;403:667–82. https://doi.org/10.1016/S0140-6736(23)02576-X.
4. Ferreira-de-Lima VH, Lima-Camara TN. Natural vertical transmission of dengue virus in Aedes aegypti and Aedes albopictus: a systematic review. Parasit Vectors. 2018;11:77. https://doi.org/10.1186/s13071-018-2643-9.
5. Lequime S, Lambrechts L. Vertical transmission of arboviruses in mosquitoes: a historical perspective. Infect Genet Evol J Mol Epidemiol Evol Genet Infect Dis. 2014;28:681–90. https://doi.org/10.1016/j.meegid.2014.07.025.
6. Domingo E, Schuster P. What Is a Quasispecies? Historical Origins and Current Scope. Curr Top Microbiol Immunol. 2016;392:1–22. https://doi.org/10.1007/82_2015_453.
7. Schuster P. Quasispecies on Fitness Landscapes. Curr Top Microbiol Immunol. 2016;392:61–120. https://doi.org/10.1007/82_2015_469.
8. Hapuarachchi HC, Koo C, Kek R, Xu H, Lai YL, Liu L, et al. Intra-epidemic evolutionary dynamics of a Dengue virus type 1 population reveal mutant spectra that correlate with disease transmission. Sci Rep. 2016;6:22592. https://doi.org/10.1038/srep22592.
9. Behura SK, Severson DW. Nucleotide substitutions in dengue virus serotypes from Asian and American countries: insights into intracodon recombination and purifying selection. BMC Microbiol. 2013;13:37. https://doi.org/10.1186/1471-2180-13-37.
10. Holmes EC. Patterns of intra- and interhost nonsynonymous variation reveal strong purifying selection in dengue virus. J Virol. 2003;77:11296–8. https://doi.org/10.1128/jvi.77.20.11296-11298.2003.
11. Lequime S, Fontaine A, Ar Gouilh M, Moltini-Conclois I, Lambrechts L, Genetic, Drift. Purifying Selection and Vector Genotype Shape Dengue Virus Intra-host Genetic Diversity in Mosquitoes. PLoS Genet. 2016;12:e1006111. https://doi.org/10.1371/journal.pgen.1006111.
12. Carrillo-Valenzo E, Danis-Lozano R, Velasco-Hernández JX, Sánchez-Burgos G, Alpuche C, López I, et al. Evolution of dengue virus in Mexico is characterized by frequent lineage replacement. Arch Virol. 2010;155:1401–12. https://doi.org/10.1007/s00705-010-0721-1.

13. Duong V, Simmons C, Gavotte L, Viari A, Ong S, Chantha N, et al. Genetic diversity and lineage dynamic of dengue virus serotype 1 (DENV-1) in Cambodia. Infect Genet Evol J Mol Epidemiol Evol Genet Infect Dis. 2013;15:59–68. https://doi.org/10.1016/j.meegid.2011.06.019.
14. Vu TTH, Holmes EC, Duong V, Nguyen TQ, Tran TH, Quail M, et al. Emergence of the Asian 1 genotype of dengue virus serotype 2 in viet nam: in vivo fitness advantage and lineage replacement in South-East Asia. PLoS Negl Trop Dis. 2010;4:e757. https://doi.org/10.1371/journal.pntd.0000757.
15. Phadungsombat J, Nakayama EE, Shioda T. Unraveling Dengue Virus Diversity in Asia: An Epidemiological Study through Genetic Sequences and Phylogenetic Analysis. Viruses. 2024;16:1046. https://doi.org/10.3390/v16071046.
16. O'Connor O, Ou TP, Aubry F, Dabo S, Russet S, Girault D, et al. Potential role of vector-mediated natural selection in dengue virus genotype/lineage replacements in two epidemiologically contrasted settings. Emerg Microbes Infect. 2021;10:1346–57. https://doi.org/10.1080/22221751.2021.1944789.
17. Ribeiro GS, Hamer GL, Diallo M, Kitron U, Ko AI, Weaver SC. Influence of herd immunity in the cyclical nature of arboviruses. Curr Opin Virol. 2020;40:1–10. https://doi.org/10.1016/j.coviro.2020.02.004.
18. Chen L, Zhang X, Guo X, Peng W, Zhu Y, Wang Z, et al. Neighboring mutation-mediated enhancement of dengue virus infectivity and spread. EMBO Rep. 2022;23:e55671. https://doi.org/10.15252/embr.202255671.
19. Maduranga S, Valencia BM, Sigera C, Weeratunga P, Fernando D, Rajapakse S, et al. DENcode: A model for haplotype-informed transmission probability of dengue virus. PLoS Comput Biol. 2026;22:e1014316. https://doi.org/10.1371/journal.pcbi.1014316.
20. Hapuarachchi HC, Koo C, Rajarethinam J, Chong C-S, Lin C, Yap G, et al. Epidemic resurgence of dengue fever in Singapore in 2013–2014: A virological and entomological perspective. BMC Infect Dis. 2016;16:300. https://doi.org/10.1186/s12879-016-1606-z.
21. Rajarethinam J, Ang L-W, Ong J, Ycasas J, Hapuarachchi HC, Yap G, et al. Dengue in Singapore from 2004 to 2016: Cyclical Epidemic Patterns Dominated by Serotypes 1 and 2. Am J Trop Med Hyg. 2018;99:204–10. https://doi.org/10.4269/ajtmh.17-0819.
22. Low S-L, Lam S, Wong W-Y, Teo D, Ng L-C, Tan L-K. Dengue seroprevalence of healthy adults in Singapore: serosurvey among blood donors, 2009. Am J Trop Med Hyg. 2015;93:40–5. https://doi.org/10.4269/ajtmh.14-0671.
23. Ong J, Chong C-S, Yap G, Lee C, Abdul Razak MA, Chiang S, et al. Gravitrap deployment for adult Aedes aegypti surveillance and its impact on dengue cases. PLoS Negl Trop Dis. 2020;14:e0008528. https://doi.org/10.1371/journal.pntd.0008528.
24. Wong WJ, Tan CH, Verkaik MG, Ng LC, Hoffmann AA, Chong C-S. Suppression of Aedes aegypti may not affect sympatric Aedes albopictus populations: findings from two years of entomological surveillance in Singapore. Sci Rep. 2025;15:2253. https://doi.org/10.1038/s41598-025-86139-z.
25. Ho SH, Lim JT, Ong J, Hapuarachchi HC, Sim S, Ng LC. Singapore's 5 decades of dengue prevention and control-Implications for global dengue control. PLoS Negl Trop Dis. 2023;17:e0011400.

https://doi.org/10.1371/journal.pntd.0011400.

26. Koo C, Tien WP, Xu H, Ong J, Rajarethinam J, Lai YL, et al. Highly Selective Transmission Success of Dengue Virus Type 1 Lineages in a Dynamic Virus Population: An Evolutionary and Fitness Perspective. iScience. 2018;6:38–51. https://doi.org/10.1016/j.isci.2018.07.008.
27. Tan C-H, Wong P-SJ, Li M-ZI, Vythilingam I, Ng L-C. Evaluation of the Dengue NS1 Ag Strip® for detection of dengue virus antigen in Aedes aegypti (Diptera: Culicidae). Vector Borne Zoonotic Dis. 2011;11:789–92. https://doi.org/10.1089/vbz.2010.0028.
28. Rambaut A, Lam TT, Max Carvalho L, Pybus OG. Exploring the temporal structure of heterochronous sequences using TempEst (formerly Path-O-Gen). Virus Evol. 2016;2:vew007. https://doi.org/10.1093/ve/vew007.
29. Minh BQ, Schmidt HA, Chernomor O, Schrempf D, Woodhams MD, Von Haeseler A, et al. IQ-TREE 2: New Models and Efficient Methods for Phylogenetic Inference in the Genomic Era. Mol Biol Evol. 2020;37:1530–4. https://doi.org/10.1093/molbev/msaa015.
30. Baele G, Ji X, Hassler GW, McCrone JT, Shao Y, Zhang Z, et al. BEAST X for Bayesian phylogenetic, phylogeographic and phylodynamic inference. Nat Methods. 2025;22:1653–6. https://doi.org/10.1038/s41592-025-02751-x.
31. Carpenter B, Gelman A, Hoffman MD, Lee D, Goodrich B, Betancourt M, et al. Stan: A Probabilistic Programming Language. J Stat Softw. 2017;76:1. https://doi.org/10.18637/jss.v076.i01.
32. Katoh K, Standley DM. MAFFT multiple sequence alignment software version 7: improvements in performance and usability. Mol Biol Evol. 2013;30:772–80. https://doi.org/10.1093/molbev/mst010.
33. Li W, Godzik A. Cd-hit: a fast program for clustering and comparing large sets of protein or nucleotide sequences. Bioinformatics. 2006;22:1658–9. https://doi.org/10.1093/bioinformatics/btl158.
34. Hall TA. BioEdit: a user-friendly biological sequence alignment editor and analysis program for Windows 95/98/NT. 1999;41:95–8.
35. Page AJ, Taylor B, Delaney AJ, Soares J, Seemann T, Keane JA, et al. SNP-sites: rapid efficient extraction of SNPs from multi-FASTA alignments. Microb Genomics. 2016;2:e000056. https://doi.org/10.1099/mgen.0.000056.
36. Hadfield J, Megill C, Bell SM, Huddleston J, Potter B, Callender C, et al. Nextstrain: real-time tracking of pathogen evolution. Bioinformatics. 2018;34:4121–3. https://doi.org/10.1093/bioinformatics/bty407.
37. Barnes J, Hut P. A hierarchical O(N log N) force-calculation algorithm. Nature. 1986;324:446–9. https://doi.org/10.1038/324446a0.
38. Perrone G, Unpingco J, Lu H. Network visualizations with Pyvis and VisJS. 2020. https://doi.org/10.48550/arXiv.2006.04951
39. Kosakovsky Pond SL, Poon AFY, Velazquez R, Weaver S, Hepler NL, Murrell B, et al. HyPhy 2.5—A Customizable Platform for Evolutionary Hypothesis Testing Using Phylogenies. Mol Biol Evol. 2020;37:295–9. https://doi.org/10.1093/molbev/msz197.

40. Kosakovsky Pond SL, Frost SDW. Not so different after all: a comparison of methods for detecting amino acid sites under selection. Mol Biol Evol. 2005;22:1208–22. https://doi.org/10.1093/molbev/msi105.
41. Murrell B, Moola S, Mabona A, Weighill T, Sheward D, Kosakovsky Pond SL, et al. FUBAR: a fast, unconstrained bayesian approximation for inferring selection. Mol Biol Evol. 2013;30:1196–205. https://doi.org/10.1093/molbev/mst030.
42. Murrell B, Wertheim JO, Moola S, Weighill T, Scheffler K, Kosakovsky Pond SL. Detecting individual sites subject to episodic diversifying selection. PLoS Genet. 2012;8:e1002764. https://doi.org/10.1371/journal.pgen.1002764.
43. Paradis E. pegas: an R package for population genetics with an integrated–modular approach. Bioinformatics. 2010;26:419–20. https://doi.org/10.1093/bioinformatics/btp696.
44. Naveca FG, Santiago GA, Maito RM, Ribeiro Meneses CA, do, Nascimento VA, de Souza VC et al. Reemergence of Dengue Virus Serotype 3, Brazil, 2023. Emerg Infect Dis. 2023;29:1482–4. https://doi.org/10.3201/eid2907.230595
45. Lagrave A, Enfissi A, Tirera S, Demar MP, Jaonasoa J, Carod J-F, et al. Re-Emergence of DENV-3 in French Guiana: Retrospective Analysis of Cases That Circulated in the French Territories of the Americas from the 2000s to the 2023–2024 Outbreak. Viruses. 2024;16:1298. https://doi.org/10.3390/v16081298.
46. Soe AM, Ngwe Tun MM, Nabeshima T, Myat TW, Htun MM, Lin H, et al. Emergence of a Novel Dengue Virus 3 (DENV-3) Genotype-I Coincident with Increased DENV-3 Cases in Yangon, Myanmar between 2017 and 2019. Viruses. 2021;13:1152. https://doi.org/10.3390/v13061152.
47. Costa RL, Voloch CM, Schrago CG. Comparative evolutionary epidemiology of dengue virus serotypes. Infect Genet Evol. 2012;12:309–14. https://doi.org/10.1016/j.meegid.2011.12.011.
48. Zhang C, Mammen MP, Chinnawirotpisan P, Klungthong C, Rodpradit P, Monkongdee P, et al. Clade Replacements in Dengue Virus Serotypes 1 and 3 Are Associated with Changing Serotype Prevalence. J Virol. 2005;79:15123–30. https://doi.org/10.1128/JVI.79.24.15123-15130.2005.
49. Schober P, Boer C, Schwarte LA. Correlation Coefficients: Appropriate Use and Interpretation. Anesth Analg. 2018;126:1763–8. https://doi.org/10.1213/ANE.0000000000002864.
50. Tajima F. Statistical analysis of DNA polymorphism. Idengaku Zasshi. 1993;68:567–95. https://doi.org/10.1266/jjg.68.567.
51. Steinhauer DA, Domingo E, Holland JJ. Lack of evidence for proofreading mechanisms associated with an RNA virus polymerase. Gene. 1992;122:281–8. https://doi.org/10.1016/0378-1119(92)90216-c.
52. Sanjuán R, Domingo-Calap P. Mechanisms of viral mutation. Cell Mol Life Sci CMLS. 2016;73:4433–48. https://doi.org/10.1007/s00018-016-2299-6.
53. Bifani AM, Siriphanitchakorn T, Choy MM. Intra-Host Diversity of Dengue Virus in Mosquito Vectors. Front Cell Infect Microbiol. 2022;12:888804. https://doi.org/10.3389/fcimb.2022.888804.

54. Parameswaran P, Wang C, Trivedi SB, Eswarappa M, Montoya M, Balmaseda A, et al. Intrahost Selection Pressures Drive Rapid Dengue Virus Microevolution in Acute Human Infections. Cell Host Microbe. 2017;22:400–e4105. https://doi.org/10.1016/j.chom.2017.08.003.
55. Kurosu T. Quasispecies of dengue virus. Trop Med Health. 2011;39(4 Suppl):29–36. https://doi.org/10.2149/tmh.2011-S02.
56. Nonyong P, Ekalaksananan T, Phanthanawiboon S, Overgaard HJ, Alexander N, Thaewnongiew K, et al. Intrahost Genetic Diversity of Dengue Virus in Human Hosts and Mosquito Vectors under Natural Conditions Which Impact Replicative Fitness In Vitro. Viruses. 2023;15:982. https://doi.org/10.3390/v15040982.
57. Liang X, Tan CH, Sun Q, Zhang M, Wong PSJ, Li MI, et al. Wolbachia wAlbB remains stable in Aedes aegypti over 15 years but exhibits genetic background-dependent variation in virus blocking. PNAS Nexus. 2022;1:pgac203. https://doi.org/10.1093/pnasnexus/pgac203.
58. Moreira LA, Iturbe-Ormaetxe I, Jeffery JA, Lu G, Pyke AT, Hedges LM, et al. A Wolbachia symbiont in Aedes aegypti limits infection with dengue, Chikungunya, and Plasmodium. Cell. 2009;139:1268–78. https://doi.org/10.1016/j.cell.2009.11.042.
59. Wang L, Huang AT, Katzelnick LC, Lefrancq N, Escoto AC, Duret L, et al. Antigenic distance between primary and secondary dengue infections correlates with disease risk. Sci Transl Med. 2024;16:eadk3259. https://doi.org/10.1126/scitranslmed.adk3259.
60. Wang L, Huang AT, Katzelnick LC, Lefrancq N, Escoto AC, Duret L, et al. Antigenic diversity and dengue disease risk. Res Sq. 2023. https://doi.org/10.21203/rs.3.rs-3214507/v1. :rs.3.rs-3214507.
61. Katzelnick LC, Coello Escoto A, Huang AT, Garcia-Carreras B, Chowdhury N, Maljkovic Berry I, et al. Antigenic evolution of dengue viruses over 20 years. Science. 2021;374:999–1004. https://doi.org/10.1126/science.abk0058.
62. Mustafa MS, Rastogi V, Gupta RK, Jain S, Singh PMP, Gupta A. Wolbachia: The selfish Trojan Horse in dengue control. Med J Armed Forces India. 2016;72:373–6. https://doi.org/10.1016/j.mjafi.2015.07.002.
63. Ko H-Y, Li Y-T, Chao D-Y, Chang Y-C, Li Z-RT, Wang M, et al. Inter- and intra-host sequence diversity reveal the emergence of viral variants during an overwintering epidemic caused by dengue virus serotype 2 in southern Taiwan. PLoS Negl Trop Dis. 2018;12:e0006827. https://doi.org/10.1371/journal.pntd.0006827.
64. Rodriguez-Roche R, Blanc H, Bordería AV, Díaz G, Henningsson R, Gonzalez D, et al. Increasing Clinical Severity during a Dengue Virus Type 3 Cuban Epidemic: Deep Sequencing of Evolving Viral Populations. J Virol. 2016;90:4320–33. https://doi.org/10.1128/JVI.02647-15.
65. Finch E, Chang C-C, Kucharski A, Sim S, Ng L-C, Lowe R. Climate variation and serotype competition drive dengue outbreak dynamics in Singapore. Nat Commun. 2025;16:11364. https://doi.org/10.1038/s41467-025-66411-6.
66. Lim JT, Chong C-S, Chang C-C, Mailepessov D, Dickens B, Lai YL, et al. Dengue Suppression by Male Wolbachia-Infected Mosquitoes. N Engl J Med. 2026;394:1175–83.

https://doi.org/10.1056/NEJMoa2503304.

67. Lim JT, Lee VJ, Tan CH, Chong C-S, Vasquez K, Ng LC. Combating dengue using male Wolbachia-infected mosquitoes-lessons from Singapore's experience. Lancet Reg Health West Pac. 2026;69:101841. https://doi.org/10.1016/j.lanwpc.2026.101841.
68. Pollett S, Melendrez MC, Maljkovic Berry I, Duchêne S, Salje H, Cummings D, a. T, et al. Understanding dengue virus evolution to support epidemic surveillance and counter-measure development. Infect Genet Evol J Mol Epidemiol Evol Genet Infect Dis. 2018;62:279–95. https://doi.org/10.1016/j.meegid.2018.04.032.
69. Finch E, Chang C, Kucharski A, Sim S, Ng L-C, Lowe R. Climate variation and serotype competition drive dengue outbreak dynamics in Singapore. Nat Commun. 2025;16:11364. https://doi.org/10.1038/s41467-025-66411-6.
70. Tan LK, Low SL, Sun H, Shi Y, Liu L, Lam S, et al. Force of Infection and True Infection Rate of Dengue in Singapore: Implications for Dengue Control and Management. Am J Epidemiol. 2019;188:1529–38. https://doi.org/10.1093/aje/kwz110.
71. Yung C-F, Lee K-S, Thein T-L, Tan L-K, Gan VC, Wong JGX, et al. Dengue serotype-specific differences in clinical manifestation, laboratory parameters and risk of severe disease in adults, singapore. Am J Trop Med Hyg. 2015;92:999–1005. https://doi.org/10.4269/ajtmh.14-0628.
72. Long H, Chen Y, Feng J, Chen J, Zhang X, Han W, et al. Annual global dengue dynamics are related to multi-source factors revealed by a machine learning prediction analysis. PLoS Negl Trop Dis. 2025;19:e0013232. https://doi.org/10.1371/journal.pntd.0013232.
73. Yu X, Cheng G. Contribution of phylogenetics to understanding the evolution and epidemiology of dengue virus. Anim Models Exp Med. 2022;5:410–7. https://doi.org/10.1002/ame2.12283.
74. Tan CH, Hapuarachchi HC, Tan LK, Wong PSJ, Li MZI, Wong WY, et al. Lineage Replacement Associated with Fitness Gain in Mammalian Cells and Aedes aegypti: A Catalyst for Dengue Virus Type 2 Transmission. Microorganisms. 2022;10:1100. https://doi.org/10.3390/microorganisms10061100.
75. Chan M, Johansson MA. The incubation periods of Dengue viruses. PLoS ONE. 2012;7:e50972. https://doi.org/10.1371/journal.pone.0050972.
76. Tjaden NB, Thomas SM, Fischer D, Beierkuhnlein C. Extrinsic Incubation Period of Dengue: Knowledge, Backlog, and Applications of Temperature Dependence. PLoS Negl Trop Dis. 2013;7:e2207. https://doi.org/10.1371/journal.pntd.0002207.
77. Brass DP, Cobbold CA, Purse BV, Ewing DA, Callaghan A, White SM. Role of vector phenotypic plasticity in disease transmission as illustrated by the spread of dengue virus by Aedes albopictus. Nat Commun. 2024;15:7823. https://doi.org/10.1038/s41467-024-52144-5.
78. Makau DN, Lycett S, Michalska-Smith M, Paploski IAD, Cheeran MC-J, Craft ME, et al. Ecological and evolutionary dynamics of multi-strain RNA viruses. Nat Ecol Evol. 2022;6:1414–22. https://doi.org/10.1038/s41559-022-01860-6.

79. Chambers TJ, Hahn CS, Galler R, Rice CM. Flavivirus genome organization, expression, and replication. Annu Rev Microbiol. 1990;44:649–88. https://doi.org/10.1146/annurev.mi.44.100190.003245.
80. Incicco JJ, Cababie LA, Sarto C, Adler NS, Amrein F, Mikkelsen E, et al. Thermodynamic and mechanistic analysis of the functional properties of dengue virus NS3 helicase. Biophys Rev. 2023;15:591–600. https://doi.org/10.1007/s12551-023-01101-5.
81. Perera DR, Ranadeva ND, Sirisena K, Wijesinghe KJ. Roles of NS1 Protein in Flavivirus Pathogenesis. ACS Infect Dis. 2024;10:20–56. https://doi.org/10.1021/acsinfecdis.3c00566.
82. Zeng Q, Liu J, Hao C, Zhang B, Zhang H. Making sense of flavivirus non-strctural protein 1 in innate immune evasion and inducing tissue-specific damage. Virus Res. 2023;336:199222. https://doi.org/10.1016/j.virusres.2023.199222.
83. Zhang S, He Y, Wu Z, Wang M, Jia R, Zhu D, et al. Secretory pathways and multiple functions of nonstructural protein 1 in flavivirus infection. Front Immunol. 2023;14:1205002. https://doi.org/10.3389/fimmu.2023.1205002.
84. Domingo E, Perales C. Viral quasispecies. PLoS Genet. 2019;15:e1008271. https://doi.org/10.1371/journal.pgen.1008271.
85. Wang W-K, Lin S-R, Lee C-M, King C-C, Chang S-C. Dengue type 3 virus in plasma is a population of closely related genomes: quasispecies. J Virol. 2002;76:4662–5. https://doi.org/10.1128/jvi.76.9.4662-4665.2002.

Figures

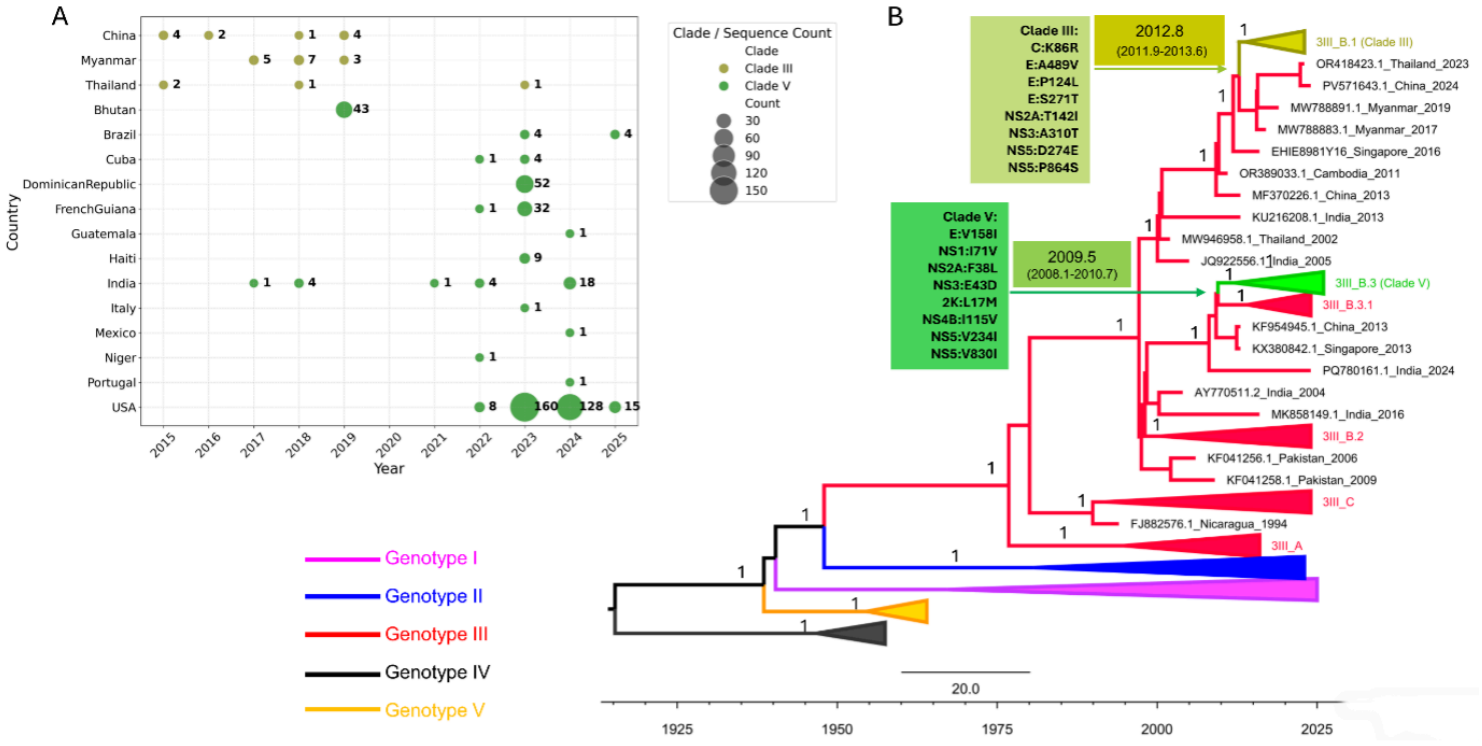


Figure 1

Genetic relationship of clade III and clade V.A) Temporal distribution of complete coding sequences possessing amino acid substitution profile of each clade reported elsewhere. All sequences of respective clades possess the substitutions in each profile (“fixed”) that are also possessed by sequences reported from other countries (n=1,481), though genetically not identical. The reporting time frame and the number of sequences is indicated in brackets. B) Bayesian phylogeny of DENV-3. The tree was constructed by using BEAST 10.5.0 software suite (Baele et al., 2025) and included complete coding sequences of clade III (n=134) and clade V (n=37). The analysis also included 179 complete coding sequences retrieved from NCBI database to represent different genotypes of DENV-3. The amino acid substitution profiles and tMRCA (95% HPD values in brackets) of clade III and clade V are shown in shaded test boxes. Genotypes are colour coded.

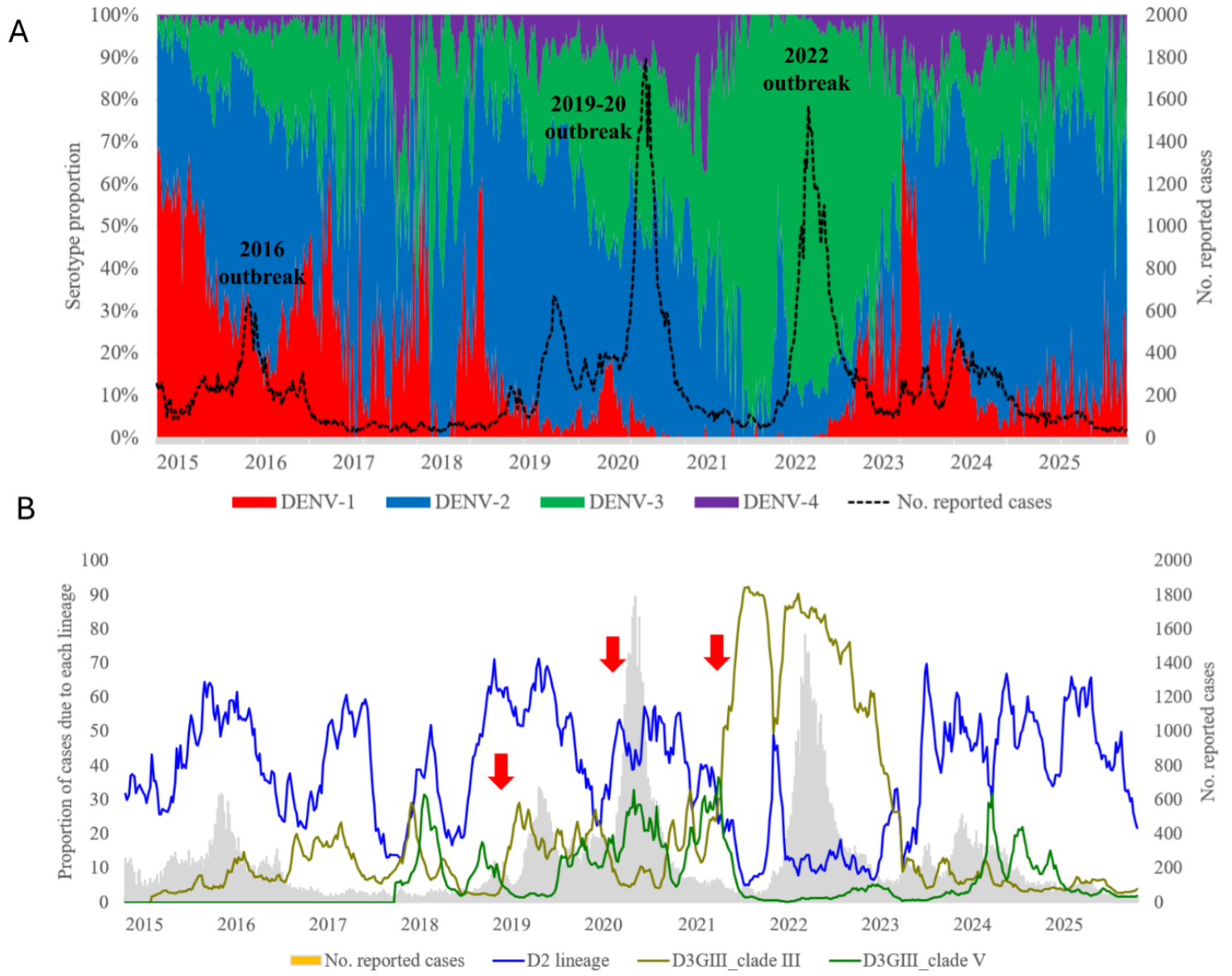


Figure 2

DENV cases, serotypes and lineage dominance. A). Longitudinal pattern of DENV serotypes and cases in Singapore from 2015 to 2025. B). Longitudinal fluctuation of lineage dominance from 2015 to 2025. Arrows indicate crossing points of clades III and V's relative dominance. D2 = DENV-2; D3 = DENV-3; GIII = Genotype III.

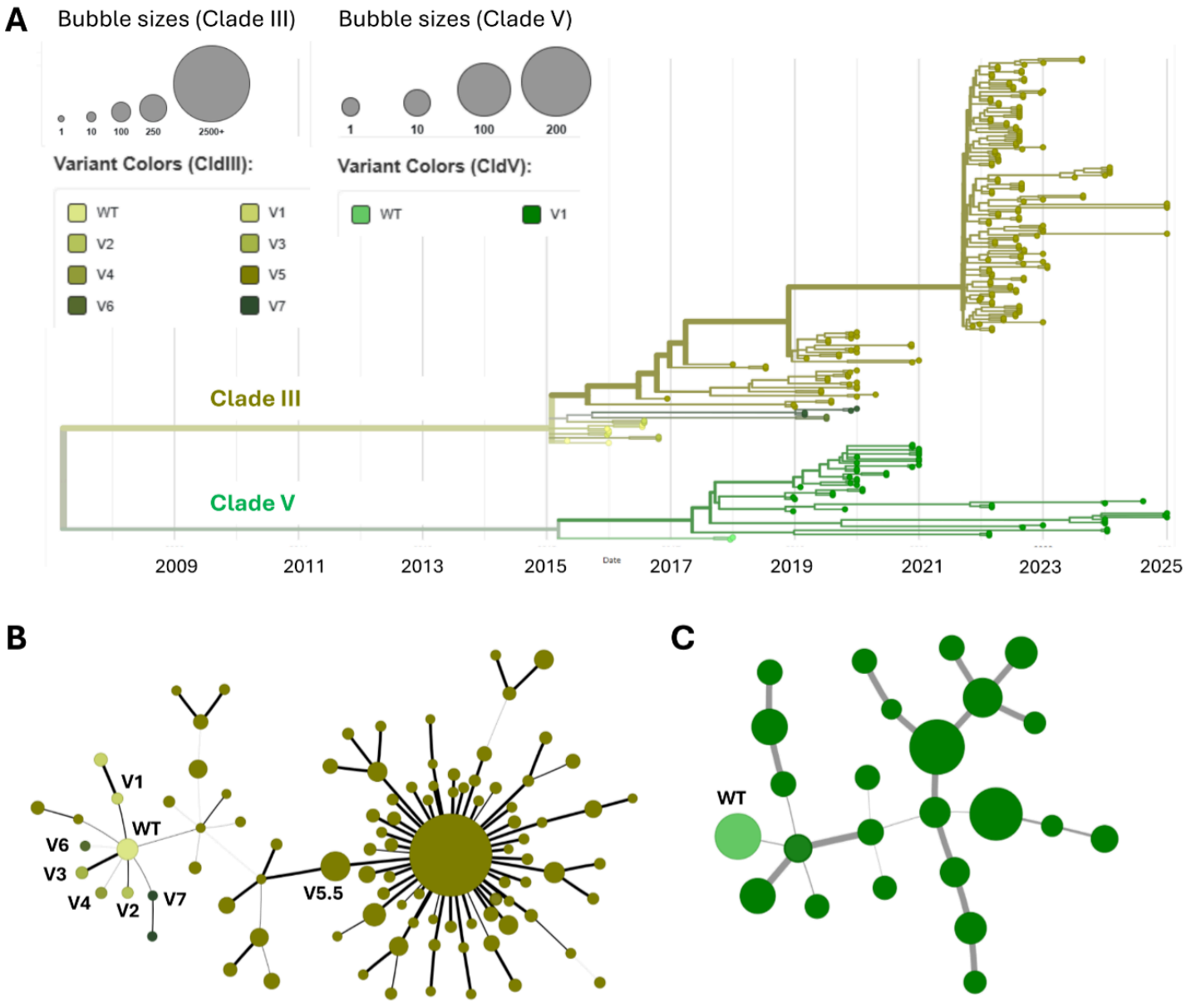


Figure 3

Haplotype tree and network of clades III and V. A) The maximum likelihood phylogenetic analysis included complete *E* gene sequences of clade III (n=192) and clade V (n=48), representative of the WT and all haplotypes detected. The analysis was conducted using Nextstrain pipeline [36]. The tree illustrates the progressive evolution of different variants of clades III and V. B) Haplotype network of clade III C) Haplotype network of clade V. The minimum spanning tree (MST) networks illustrate genetic relationships between haplotypes and dominant variants of each clade.

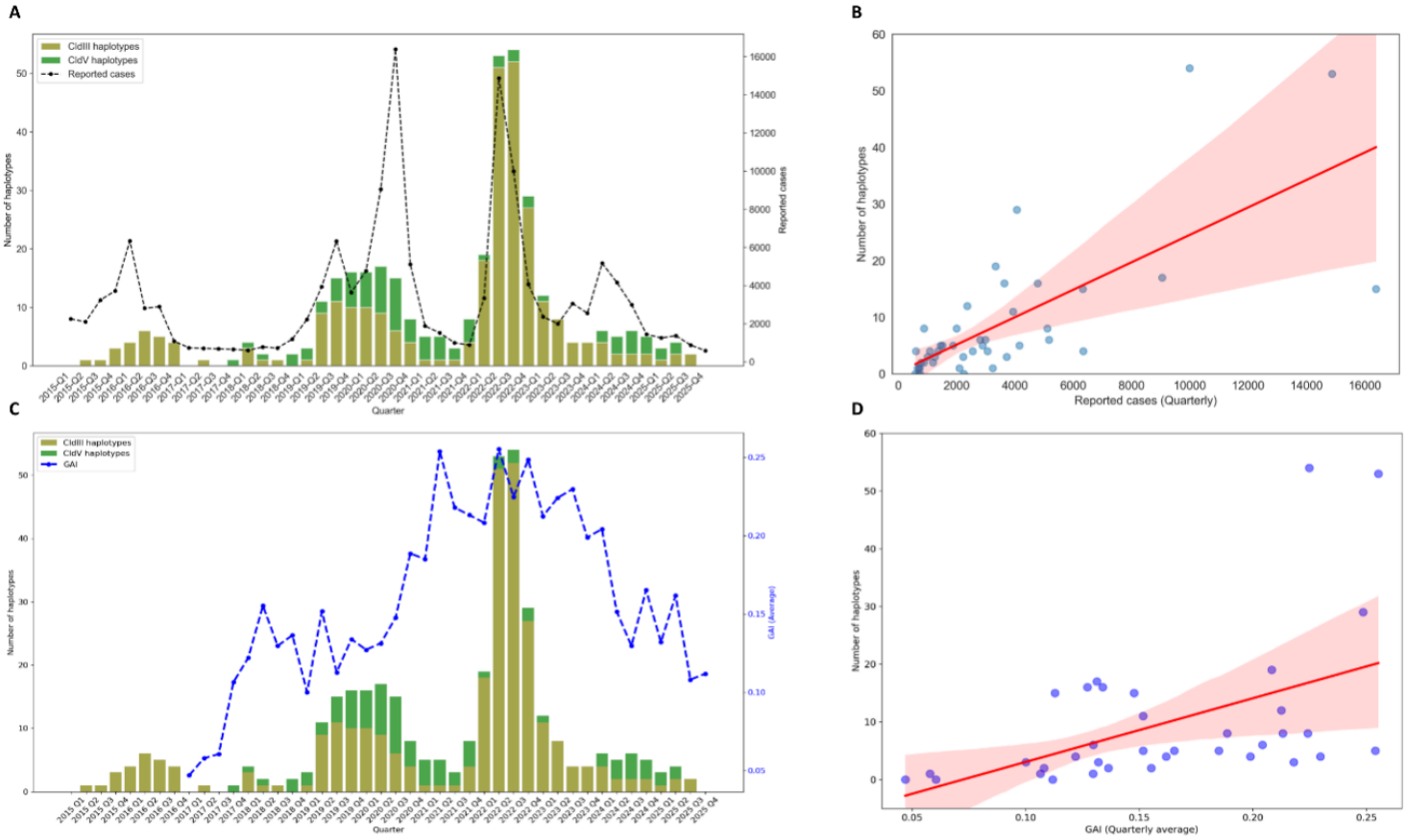


Figure 4

Longitudinal distribution of dengue cases, vector index and the number of haplotypes of each clade from 2015 to 2025. A). Temporal distribution of number of cases and haplotypes B). Correlation between number of cases and haplotypes C). Temporal distribution of number of cases and Gravitrap *Ae. aegypti* Index (GAI) D). Correlation between GAI and haplotypes. The graph illustrates that the highest number of haplotypes coincided with peaks in cases and GAI that indicate high transmission periods.

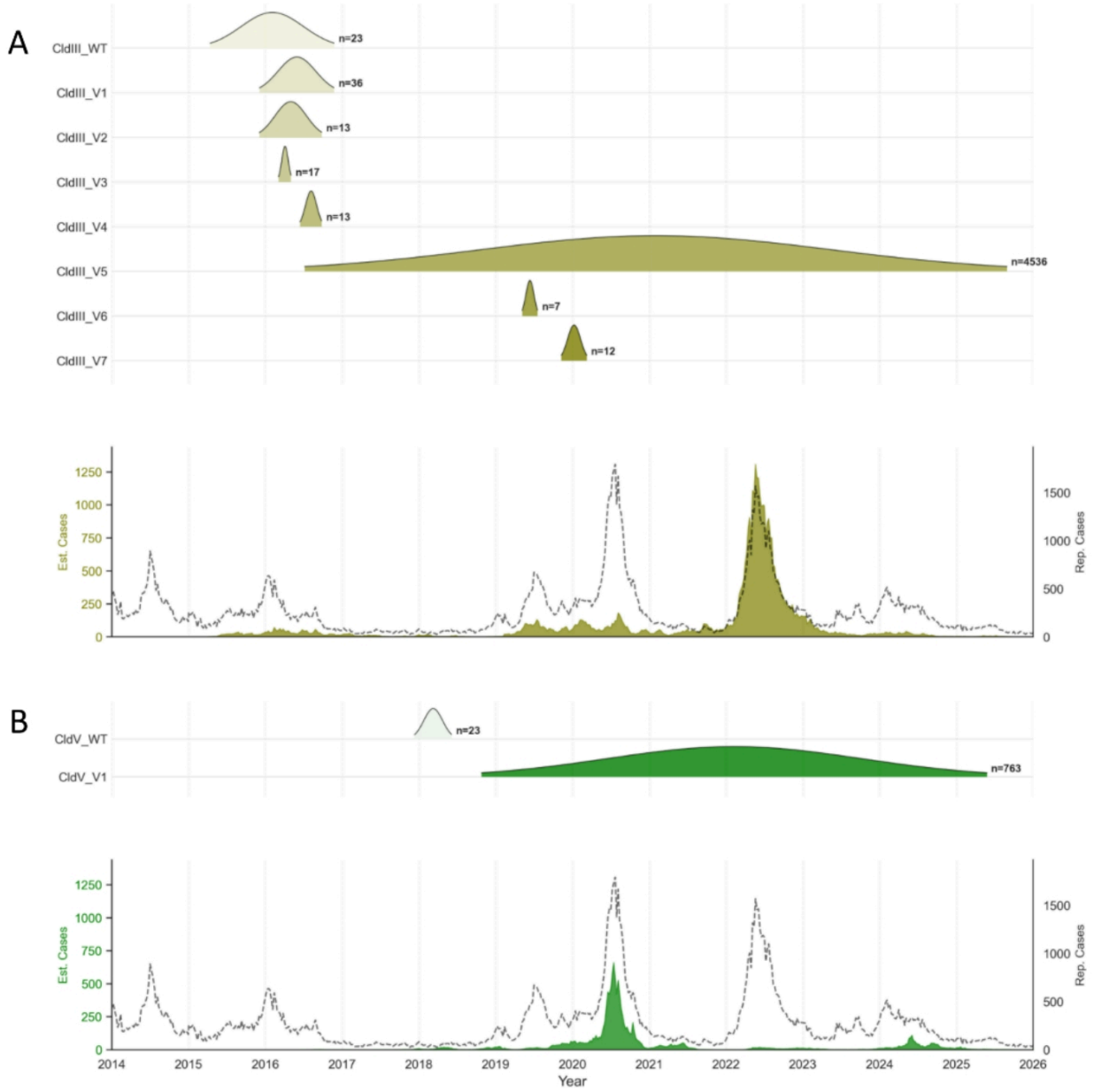


Figure 5

Longitudinal dynamics of each clade, variants and reported cases. A) Clade III B) Clade V. Estimated number of cases due to each clade in comparison to total cases reported highlights their alternative dominance during 2019-2020 and 2022 outbreaks. V = variant; WT = Wild type.

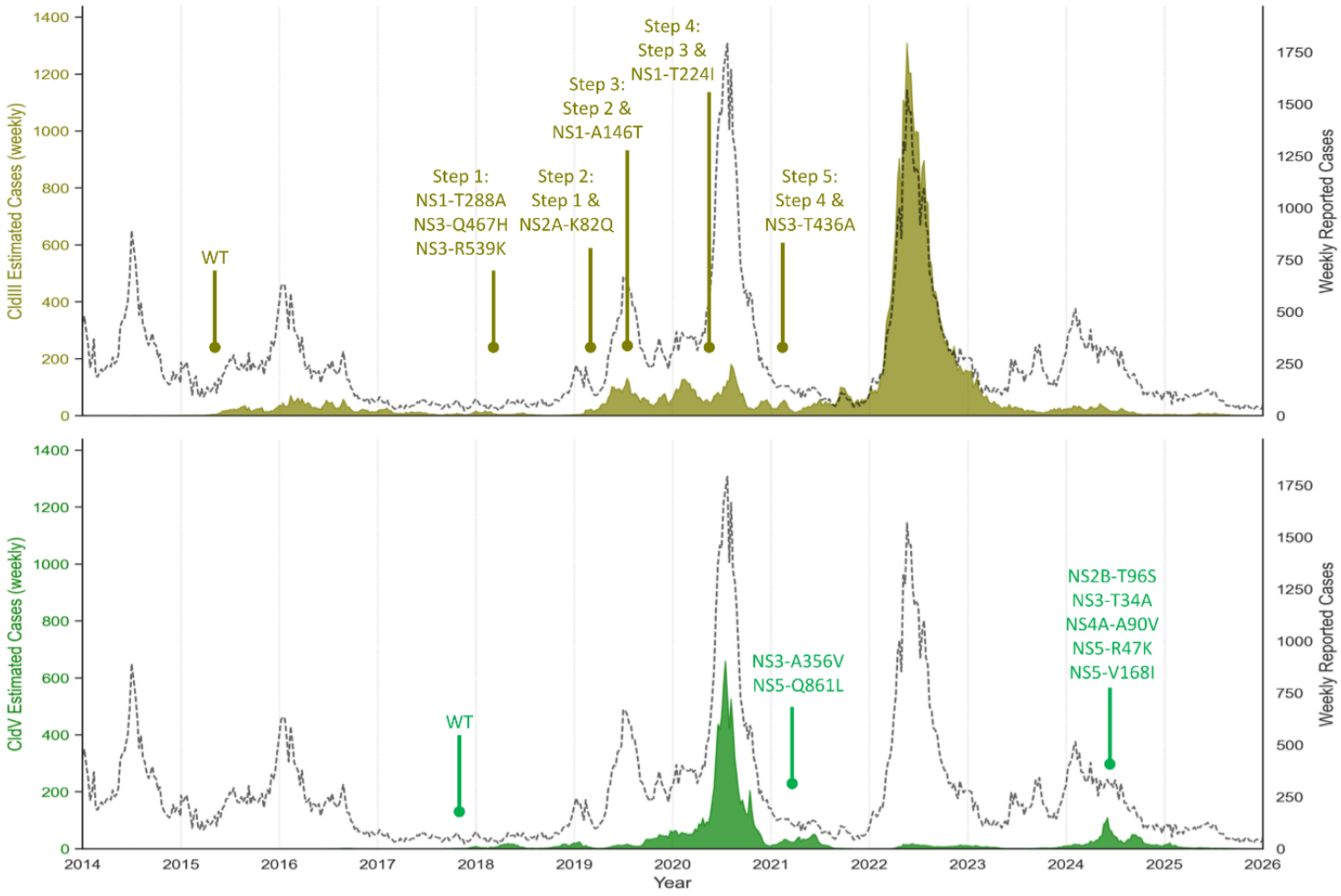


Figure 6

Temporal analysis of the emergence of non-synonymous substitutions in each clade. The arrows indicate the time of first detection of each substitution that appeared in a stepladder pattern in clade III, in contrast to the introduction-dominated pattern reflected in weaker in-situ accumulation signal in clade V. WT=wild type, NS=non-structural.

Supplementary Files

This is a list of supplementary files associated with this preprint. Click to download.

- AdditionalFiles.docx